

Run-of-river dam designing and modelling of its influence on the propagation of floods from the Davo River to the drinking water production station in Gueyo (Côte d'Ivoire)

KOUASSI Kouakou Lazare¹, KOUADIO Zilé Alex¹, KOUAME Yao Morton¹, YAO Affoué Berthe¹, OUEDE Gla Blaise¹, and KOUADIO Koffi Prosper²

¹University Jean Lorougnon Guédé, BP 150 Daloa, Côte d'Ivoire

²National Bureau of Technical Studies and Development (BNETD), 04 BP 945 Abidjan 04, Côte d'Ivoire

Copyright © 2019 ISSR Journals. This is an open access article distributed under the *Creative Commons Attribution License*, which permits unrestricted use, distribution, and reproduction in any medium, provided the original work is properly cited.

ABSTRACT: The construction of hydraulic structures on watercourses modifies the flow conditions and the extent of flood propagation zones. To do this, the installation of the structures must be preceded by models ensuring the correct dimensioning of the structures and their influence on the hydrological functioning of the watercourse. This study used hydrometric data, satellite images and cartographic data to design a run-of-river dam and model its influence on the propagation of floods from the Davo River to the drinking water production station in Gueyo (Côte d'Ivoire). The dimensioning of the weir gave the following main characteristics: 2.5 m height, 1.3 m wide at the crest, 3.8 m right-of-way and 177 m long. The retention created by the presence of this weir answer the population's water needs, which are estimated at 0.19 m³/s, or 16,800 m³/day. Simulation of the behaviour of the Davo River during high water periods shows that the presence of the weir does not have a significant impact on the extent of the floodplain area.

KEYWORDS: run-of-river dam, hydrological modelling, flood propagation, Davo River, Côte d'Ivoire.

1 INTRODUCTION

The climatic variations observed in the world over the last few decades have had a major impact on the water resources of the countries of the African continent. Côte d'Ivoire is not exempt from this phenomenon [1], [2], [3], [4]. Water shortages in some localities such as Gueyo, a city in south-western Côte d'Ivoire, are forcing the population to use surface water and traditional well water, often untreated. Consumption of this water very often causes waterborne diseases such as cholera, typhoid fever, gastroenteritis and diarrhoea [3]. Thus, to overcome the problem of water shortage in Gueyo, the Ivorian state decided to build a drinking water production station in Gueyo on the Davo River. However, given the considerable decreases in flows during low-water periods, the establishment of a weir on the Davo River is necessary to mobilize a permanent water reserve in the stream bed during low-water periods in order to meet the population's water needs, estimated at 16 800 m³/day. However, the installation of a run-of-river dam has an impact on the flow regime. Hydraulic structures such as dams can dry out the downstream bed or create flooding in the project area during high water periods [5], [6], [7], [8], [9], [10]. The purpose of this study is to design a weir to maintain a sufficient water supply for the population during low water periods while minimizing the risk of flooding during high water periods through a 2D hydrodynamic model.

2 GEOGRAPHICAL AND ENVIRONMENTAL CONTEXT

The Davo River watershed is located in southwestern Côte d'Ivoire between longitudes 6°47' W to 5°69' W and latitudes 5°03' N to 6°85' N (Fig. 1). It is a sub-watershed of the Sassandra River. The basin has an area of 7025 km².

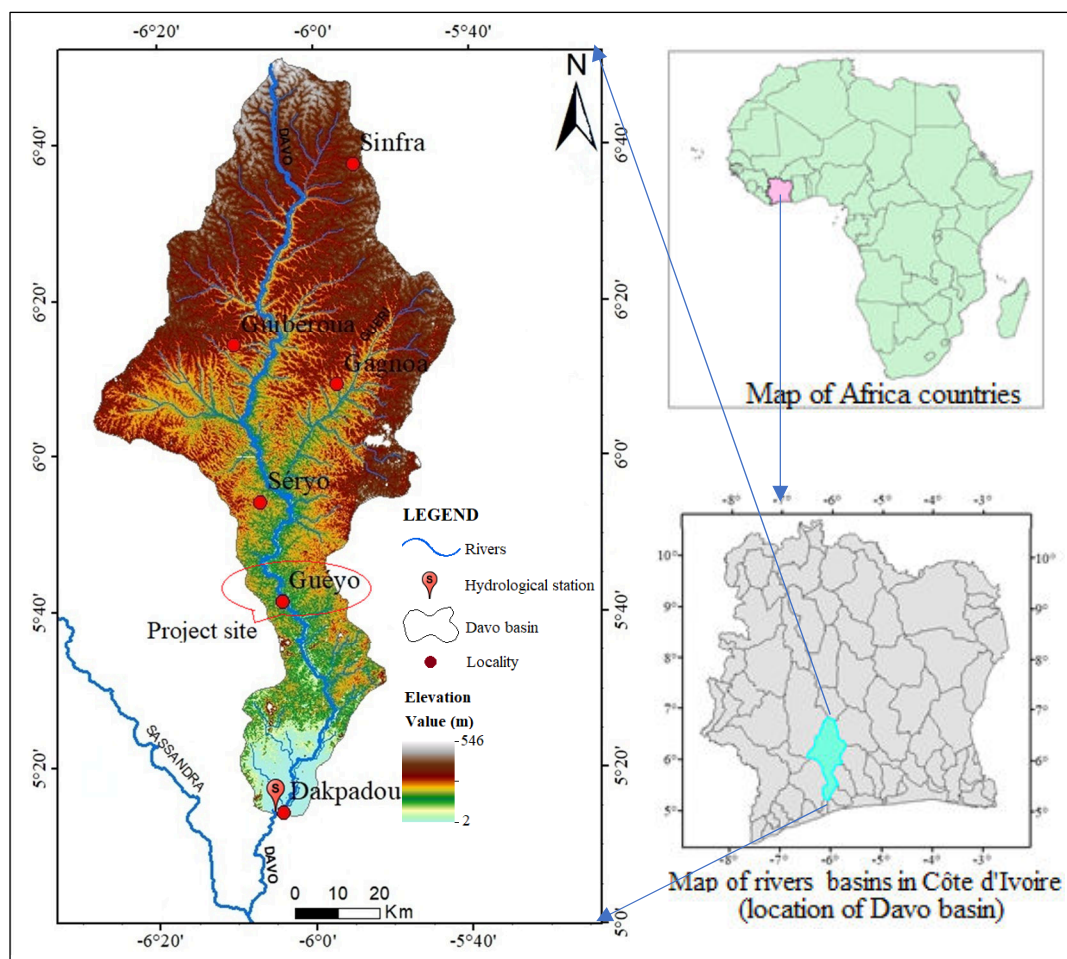


Fig. 1. Location of the Davo River Watershed

The Davo River watershed belongs to the humid tropical climate characterized by four seasons (two dry seasons and two rainy seasons): a long dry season from November to March and a short dry season from July to August; a long rainy season from April to June and a short rainy season from September to October. The maximum rainfall is observed in June with an average of 192 mm; the average annual rainfall is 1365 mm over the period 1970-2008. The average monthly temperature varies from 24.9°C to 27.8°C with an annual average of 26.4°C over the period 1970-2008. The lowest value is in August and the warmest month is February.

The study area is dominated by Proterozoic and Birmian formations. The dominant geological formations are granodiorites, granitoids, migmatites and mesozonal formations. Soils are highly desaturated ferralsols; these soils are largely occupied by the most dominant industrial crops (cocoa, coffee, rubber and oil palm).

The population of the Davo watershed is estimated at about 675,067. Economic activities are dominated by industrial agriculture (cocoa, coffee, rubber and oil palm). In terms of food crops, rice, plantain bananas, cassava and yams are the main crops. In addition to these basic products, there are vegetables (peppers, aubergines, gombos...) And fruits (citrus fruits, avocados, pineapples...).

3 MATERIALS AND METHODS

3.1 STUDY DATA

The hydrometric data used for the modelling are those of the Dakpadou hydrometric station covering the period from 1969 to 2018, at daily time steps. These data come from national services in Côte d'Ivoire and direct field measurements. The digital

elevation model (DEM) was used to extract field elevations and was used to produce thematic maps and simulate flow dynamics in Geographic Information Systems (GIS) and HEC-RAS respectively.

3.2 METHODS

3.2.1 ANALYSIS OF WATER SUPPLY/NEEDS RATIOS

The river's capacity to satisfy water needs is analyzed through parameters such as the Monthly Flow Coefficient (MFC), instream flow, and withdrawable flow. According to the water supply project for the city of Gueyo and its surrounding localities, the population's water needs are estimated at 0.19 m³/s or 16 800 m³/day. The relationship between water supply and demand was analysed through the relationship between needs and withdrawable flow. It is established with the hydrologically driest year (1983).

3.2.1.1 DETERMINATION OF LOW AND HIGH-WATER PERIODS

They are determined by calculating the monthly flow coefficient (MFC) through equation 1:

$$MFC = \frac{Q_i}{Q_M} \quad (\text{Eq. 1})$$

Q_i: average monthly flow rate

I: rank of the 12 months of the year

Q_m: average annual flow

If MFC > 1, then the month corresponds to a period of high water

If MFC < 1, then the month corresponds to a period of low water

3.2.1.2 RESERVED MONTHLY FLOW RATE

The instream flow or minimum biological flow is the minimum flow to be maintained permanently in a watercourse in way of the structure to ensure biological balances and downstream water uses. Instream flow is no longer a hydrological concept but no longer a regulatory constraint. In practice, this instream flow is equal to one-tenth of the monthly module.

3.2.1.3 MONTHLY WITHDRAWABLE FLOW RATE

This flow is obtained by subtracting the reserved flow from the monthly module. The quantity of available water being variable according to the periods of the hydrological year.

3.2.2 CALCULATION OF THE VOLUME OF THE BOWL

From the contours, half a meter per half a meter extracted using a Geographic Information System (GIS) tool, a planimage is made of the surfaces of the various contours closing on the axis of the weir (projected cross profile). The results obtained make it possible to evaluate the maximum volume of the reservoir.

In this way, the ratio between the volume of the reserve and the high of the dike can be established for different possible heights and, above all, different possible sites.

The calculation of the volume of the reservoir consists first of all in determining the surfaces S₁; S₂...; S_n of the water bodies corresponding to the contour lines at a height h apart using the tools of the geographical information system (Fig. 2). From the bottom we can thus calculate the volumes corresponding to each slice:

$$V = \frac{S_n + S_{n+1}}{2} x h \quad (\text{Eq. 2})$$

V : volume of the bowl, S_n : area according to a given contour, h : height between two curves of a given level.

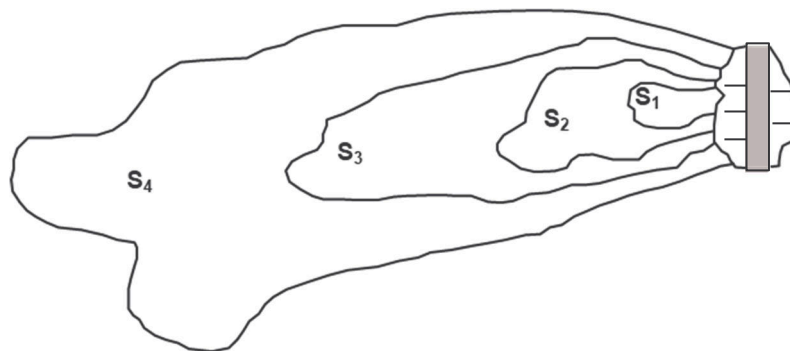


Fig. 2. Calculation of the volume of a bowl

Table 1 shows the calculation procedure of the volume of water to stored.

Table 1. Calculation of volumes by interpolation

Steps	Elevations	Surfaces	Height	Surface average	Elemental volume	Cumulative volume
0	Bottom elevation (CFD)	0	0	0	0	0
1	Bottom elevation + 1h	S ₁	H	S ₁ / 2	(S ₁ / 2) * h = V ₁	V ₁
2	Bottom elevation + 2h	S ₂	H	(S ₁ + S ₂) / 2	(S ₁ + S ₂) * h/2 = V ₂	V ₁ +V ₂
3	Bottom elevation + 3h	S ₃	H	(S ₂ + S ₃) / 2	(S ₂ + S ₃) * h/2 = V ₃	V ₁ +V ₂ +V ₃
...
N	Bottom elevation + nh	S _n	H	(S _{n-1} + S _n) / 2	(S _{n-1} + S _n) * h/2 = V _n	V _n = ∑ _i V _i

It should be noted that “Bottom elevation + nh” as indicated in the table that constitutes the normal water body rating (PEN) is also the run-of-river dam surface rating and V_n the total volume of the retention. This calculation is completed when V_n meets the population’s needs and the height of the weir does not significantly influence the spread of floods in such a way that it does not reach the position of the treatment plant and the city.

3.2.3 SIZING OF THE WEIR

The weir to be dimensioned is a run-of-river dam (flooded threshold). The specific parameters of such a weir are: height (H), crest width (b), right-of-way (E) and length of the weir (L).

3.2.3.1 WEIR HEIGHT (H)

The weir height is obtained by differentiating between the normal water body rating (PEN) and the bottom rating after stripping (CFD) of the bed at the location where the threshold was installed.

$$H = PEN - CFD \quad (\text{Eq. 3})$$

3.2.3.2 CREST WIDTH OF THE WEIR (B)

The width of the ridge must be sufficient to maintain the weir. Several empirical formulas are available. However, for this study, KNAPPEN's study is slightly modified by a factor (1/2) to design the weir:

$$B = \frac{1,65 \cdot \sqrt{H}}{2} \quad (\text{Eq. 4})$$

3.2.3.3 HOLDOVER OF THE WEIR (E)

The threshold range is determined as follows:

$$E = H + b \quad (\text{Eq. 5})$$

The longitudinal profile of the weir axis indicates the total length of the weir and is a function of the section of the major bed of the watercourse at the site of the weir (Fig. 3).

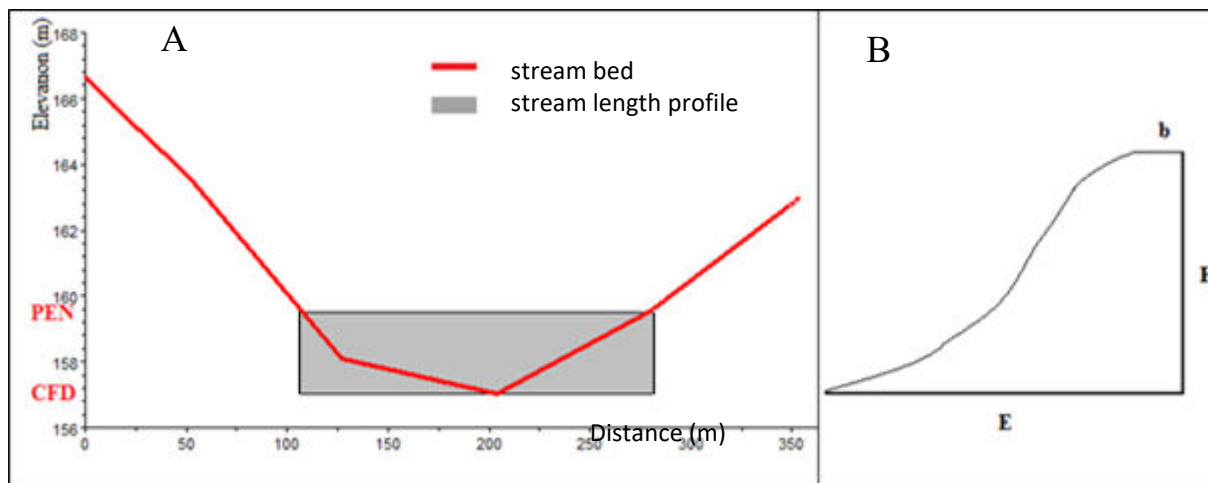


Fig. 3. Stream length profile (A) and cross profile (B) of the weir

3.2.4 SIMULATION OF STREAM DYNAMICS BEFORE AND AFTER THE INSERTION OF THE WEIR

Simulation of stream dynamics under initial and future conditions involves reproducing the behaviour of the stream in the absence of the weir and then in the presence of the weir to see the influence of its presence on the surrounding areas after its insertion into the stream bed. The dimensions of the threshold to be retained are those that maintain the extent of floodplains similar to the initial conditions of the river. This work was implemented using the HEC-RAS model.

3.2.4.1 HEC-RAS MODEL INPUT DATA

The input data of the model are:

- A digital terrain model with a resolution of 30 meters;
- A chronicle of flow data on dry and wet periods;
- A Manning coefficient of $0.05 \text{ s/m}^{1/3}$ was used; the Manning coefficient is a function of soil type, riverbed roughness, presence and absence of vegetation in the bed, and stream sinuosity [11];
- Flood hydrographs in non-permanent flow at the wedging and validation stages;
- The 20 and 100 year return period flows obtained using a frequency analysis of Gumbel's law (Table II)

Table 2. Flood quantiles and return periods of flows

Return period (year)	Probability of not exceeding (q)	Flow rate with Gumbel's law (m ³ /s)
20	0,9	320
100	0,99	419

3.2.4.2 EQUATIONS INVOLVED

The equations used are those of Saint-Venant (2D) in two directions (x; y) and in non-steady state, taking into account the time term of these equations and then in+ steady state flow, occulting the time term [12].

EQUATION OF MASS CONSERVATION

Assuming that the flow is incompressible, the unstable differential form of the mass conservation equation is:

$$\frac{\partial H}{\partial t} + \frac{\partial(hu)}{\partial x} + \frac{\partial(hv)}{\partial y} + q = 0 \text{ (Eq. 6)}$$

Where:

T: time, u and v: velocity components in the x and y directions respectively and q is a dependent flow term. In vector form, the continuity equation takes the form of:

$$\frac{\partial H}{\partial t} + \nabla \cdot hV + q = 0 \text{ (Eq. 7)}$$

Where:

V= (u,v) is the velocity vector and the differential operator

(∇): is the vector of the partial derivative operators given by $(\nabla) = (\frac{\partial}{\partial x}, \frac{\partial}{\partial y})$.

EQUATION OF MOMENTS

$$\frac{\partial u}{\partial t} + u \frac{\partial u}{\partial x} + v \frac{\partial u}{\partial y} = -g \frac{\partial H}{\partial x} + v_t \left(\frac{\partial^2 u}{\partial x^2} + \frac{\partial^2 u}{\partial y^2} \right) - c_f u \text{ (Eq. 8)}$$

$$\frac{\partial v}{\partial t} + u \frac{\partial v}{\partial x} + v \frac{\partial v}{\partial y} = -g \frac{\partial H}{\partial y} + v_t \left(\frac{\partial^2 v}{\partial x^2} + \frac{\partial^2 v}{\partial y^2} \right) - c_f v \text{ (Eq. 9)}$$

Where: u et v: speeds in Cartesian directions, g : gravitational acceleration, v_t: horizontal vortex viscosity coefficient, c_f : bottom friction coefficient.

3.2.4.3 MESHING OF THE STUDY AREA

The study area is meshed on the digital elevation model (DEM) with 6,965 cells measuring 50 m by 50 m. The weir is inserted into the model using the HEC-CRAS "inline structure data" tool (Fig. 4 et Fig.5).

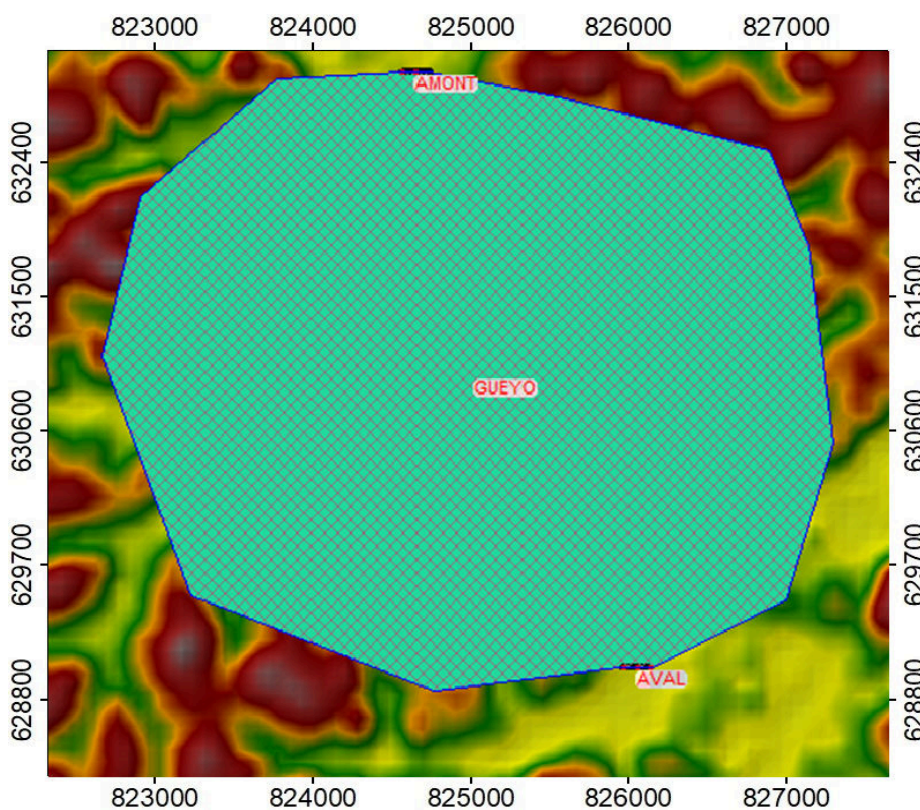


Fig. 4. Meshing of the study area

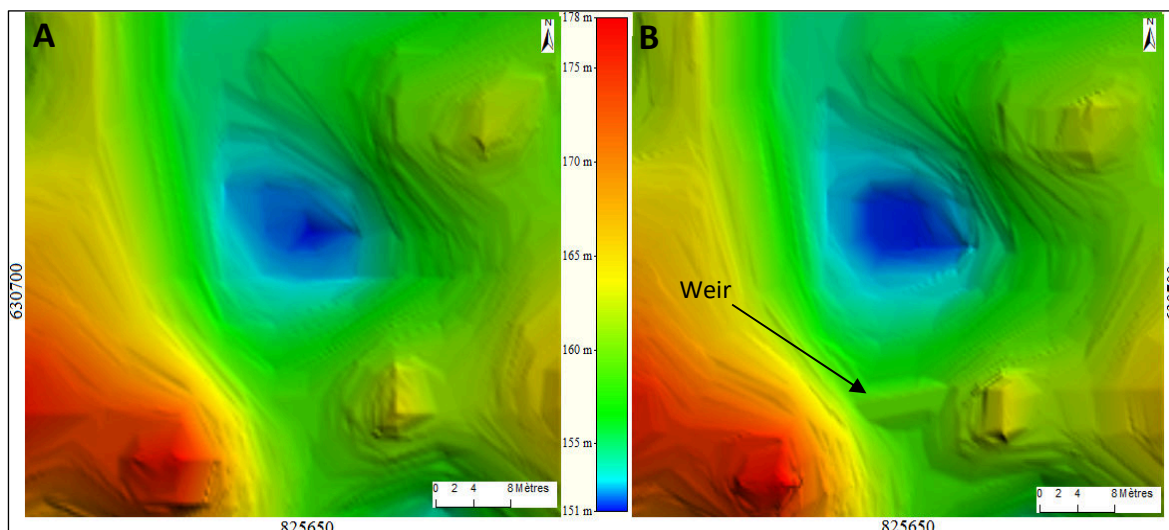


Fig. 5. Digital Elevation Model before (A) and after (B) insertion of the weir

3.2.4.4 CALIBRATION AND VALIDATION OF THE MODEL

The purpose of the calibration and validation of the model is to reproduce the behaviour of the watercourse as closely as possible. The calibration was carried out with flows from 01 January to 31 December 2003 (wet period) and validated with those from 01 January to 31 December 1992 (dry period). A Manning coefficient of $0.05 \text{ s/m}^{1/3}$ was used because of the sinuosity of the watercourse and the presence of vegetation [11], [13]. The time step used for the simulation is 2 hours. The longitudinal slope of the natural terrain (0.0002 m/m) is imposed as a downstream condition. The adjustment between the predicted and observed values was evaluated using two functions: the Nash coefficient (NTD) and the correlation coefficient (R) given by equations (9) and (10) respectively. The simulation of the flow dynamics itself is done with flows from January 01 to December 31, 2000. This period is chosen because of the extreme floods that occurred there.

$$\text{Nash coefficient : } NTD = 1 - \frac{\sqrt{\sum_{i=1}^n (q_{ci} - q_{oi})^2}}{\sqrt{\sum_{i=1}^n (q_{oi} - \bar{q}_o)^2}} \quad (\text{Eq. 10})$$

$$\text{Correlation coefficient : } R = \frac{\sum_{i=1}^n (q_{ci} - \bar{q}_c) - (q_{oi} - \bar{q}_o)}{\sqrt{\sum_{i=1}^n (q_{ci} - \bar{q}_c)^2 \sum_{i=1}^n (q_{oi} - \bar{q}_o)^2}} \quad (\text{Eq. 11})$$

Where, n represents the height of the sequence;

Q_{oi} represents the observed flow rate for step time i in m^3/s ;

Q_{ci} is the flow calculated in m^3/s for time step i;

\bar{q}_o is the mean observed flow in m^3/s .

4 RESULTS AND DISCUSSION

4.1 RESULTS

4.1.1 ANALYSIS OF THE FLOW CHARACTERISTICS OF THE DAVO RIVER

Analysis of seasonal variations in mean flow indicates that high water levels are observed from May to July and September to November (Table 3). August and December to April are the low water periods of the Davo River.

Table 3. Monthly Flow Coefficient (MFC) of the Davo River (1969-2018)

Month	Jan.	Feb.	Mar	April	May	Jun	Jul.	Ag	Sept.	Oct.	Nov.	Dec.
MFC	0.2	0.1	0.2	0.4	1.0	2.5	1.7	0.8	1.2	1.9	1.4	0.6
Periods	LW				HW		LW	HW			LW	

LW = Low Water HW = Hight Water

4.1.2 ANALYSIS OF THE WATER SUPPLY/NEEDS RATIO BEFORE AND AFTER THE INSERTION OF THE WEIR

The water supply-need relationship was analysed through the relationship between requirements and withdrawable flow for 1983 because it was particularly dry from a hydrological point of view. The results show that needs are not met during the first two months of the year, i.e. January and February under the initial flow conditions of the Davo River (Table 4).

Table 4. Water supply/water requirements ratio of the populations of Gueyo under the initial conditions of the Davo River

	Gross flows (m ³ /s)	Withdrawable flows (m ³ /s)	Withdrawable flows (m ³ /month)	Water needs (m ³ /month)	Observation
January	0.136	0.1224	327 836.16	520 800	Not satisfied
February	0.001	0.0009	2 177.28	470 400	Not satisfied
March	0.468	0.4212	1128142.1	520 800	Satisfied
April	2.61	2.349	6088608	504 000	Satisfied
May	24	21.6	57 853 440	520 800	Satisfied
June	88.5	79.65	206 452 800	504 000	Satisfied
July	44.2	39.78	106 546 752	520 800	Satisfied
August	5.93	5.337	14 294 621	520 800	Satisfied
September	5.23	4.707	12 200 544	504 000	Satisfied
October	6.54	5.886	15 765 062	520 800	Satisfied
November	7.49	6.741	17 472 672	504 000	Satisfied
December	12.4	11.16	29 890 944	520 800	Satisfied

In order to satisfy demand during January and February, a weir has been set.

4.1.3 CHARACTERISTIC OF THE WEIR

The sizing of the weir (Table IV) gave a height of 2.5 m, a crest width of 1.3 m, a right-of-way of 3.8 m and a length of 177 m. The volume of water to be retained is 670 800 m³ (Table 5).

Table 5. Weir and water retention characteristic

Parameters	Units	Values
Weir height	M	2.5
Crest width of the weir	M	1.30
Weir hold	M	3.80
Weir length	M	177
Volume of the retention	M ³	670 800
Weir position	Left Bank	825556.87 W 630639.04 X
(UTM coordinates, zone 29)	Right bank	825772.89 W 630689.39 X

4.1.4 ANALYSIS OF THE WATER SUPPLY/NEEDS RATIO OF THE POPULATIONS OF GUEYO AFTER THE ESTABLISHMENT OF THE WEIR IN THE DAVO RIVER

After the insertion of the threshold, the ratio between availability and projected needs shows a total coverage of water needs every month of the year (Table 6).

Table 6. Report on water needs and water availability after the insertion of the weir

	Gross flows (m ³ /s)	Withdrawable flows (m ³ /s)	Withdrawable flows (m ³ /month)	Water needs (m ³ /month)	Observation
January	0.136	0.1224	327 836.16	520 800	Satisfied
February	0.001	0.0009	2 177.28	470 400	Satisfied
March	0.468	0.4212	1128142.1	520 800	Satisfied
April	2.61	2.349	6088608	504 000	Satisfied
May	24	21.6	57 853 440	520 800	Satisfied
June	88.5	79.65	206 452 800	504 000	Satisfied
July	44.2	39.78	106 546 752	520 800	Satisfied
August	5.93	5.337	14 294 621	520 800	Satisfied
September	5.23	4.707	12 200 544	504 000	Satisfied
October	6.54	5.886	15 765 062	520 800	Satisfied
November	7.49	6.741	17 472 672	504 000	Satisfied
December	12.4	11.16	29 890 944	520 800	Satisfied

4.1.5 SIMULATION OF STREAM DYNAMICS BEFORE AND AFTER THE INSERTION OF THE WEIR

4.1.5.1 MODEL CALIBRATION AND VALIDATION RESULTS

Comparison of the simulated and observed hydrographs shows that the model reproduces well the environmental conditions at the time of calibration. The model performance results in a correlation coefficient of 96% and a Nash coefficient of 71%. This strong correlation also shows that the model reproduces the hydrodynamic conditions of the environment well (Fig. 6a).

This performance of the model can be observed also during validation (Fig. 6b). Indeed, the comparison of hydrographs shows a good synchronism between the simulated and observed flows. This is confirmed by the speed of the variation curves of simulated and measured flows. This good correlation results in a correlation coefficient of 92% and a Nash coefficient of 60.12% at validation.

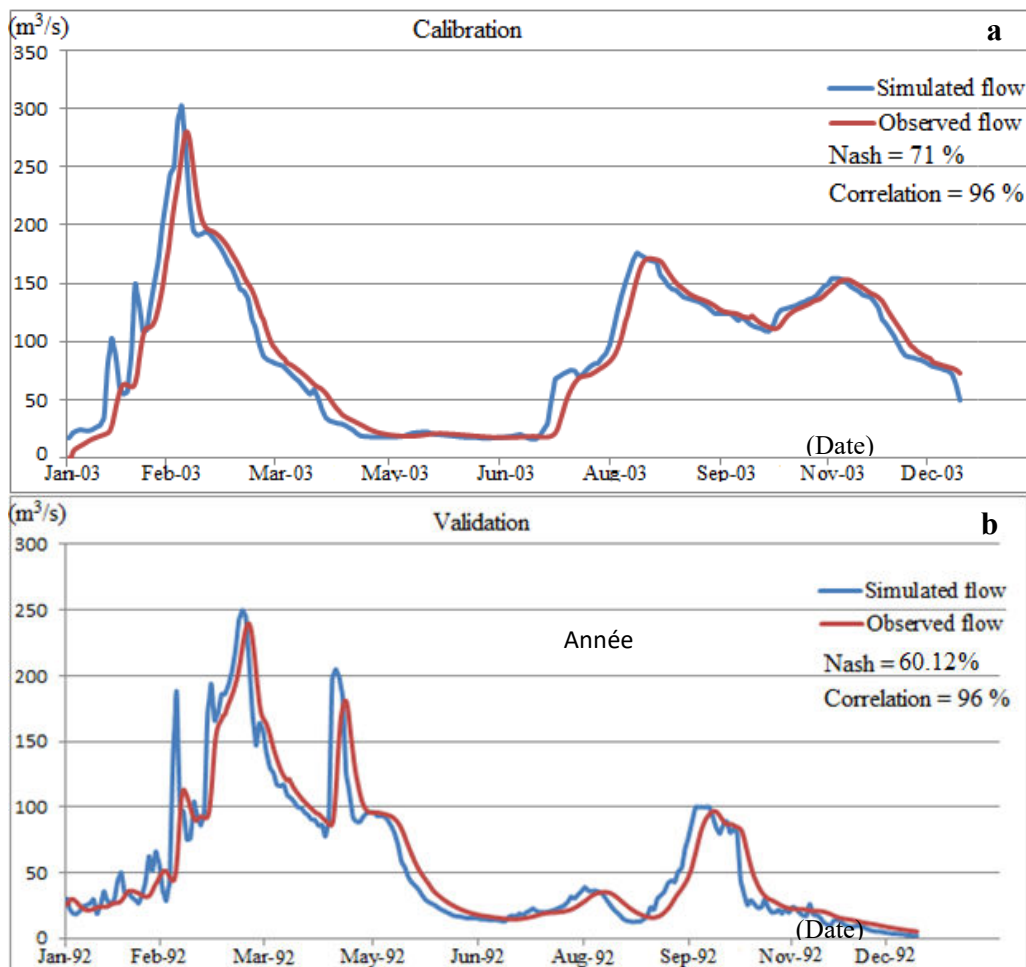


Fig. 6. Comparison of observed and simulated flows: a) calibration; b) validation (m³/s)

4.1.5.2 SIMULATION OF THE HYDROLOGICAL BEHAVIOUR OF THE DAVO RIVER BEFORE AND AFTER THE INSERTION OF THE WEIR

Fig. 7. Shows the water levels after simulation of the flows in the year 2000 in the vicinity of the town of Guéyo and the treatment plant in the absence and presence of the weir. The results show that the ratings reached by the water before and after the insertion of the threshold vary little. The maximum coasts reached before and after the insertion of the weir are 159.71 m and 159.82 m respectively in the basin and 154.85 m and 154.74 m downstream of the weir. When the threshold is present, the water level increases upstream while downstream the water level decreases.

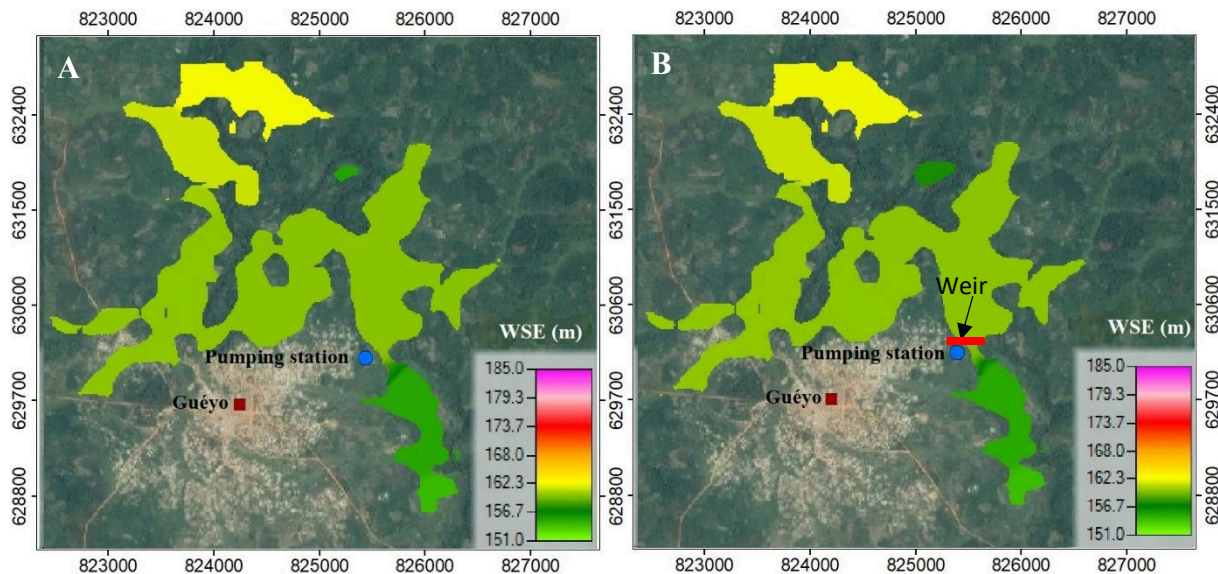


Fig. 7. Water surface elevation (WSE) before (A) and after (B) the insertion of the weir

4.1.5.3 SIMULATION OF THE WATERCOURSE AT DIFFERENT RETURN PERIODS (20 AND 100 YEARS)

Fig. 8 and Fig. 9 show water levels for return periods of 20 years and 100 years. It can be seen that, for the 20 and 100 year return periods, the maximum level reached by the river in the absence and presence of the weir are:

- In the basin (in the absence of the weir) 160.65 m and 160.93 m,
- In the basin (in the presence of the weir) 160.75 m and 161.06 m,
- Downstream (in the absence of the weir) 155.74 m and 156.1 m,
- Downstream (in the presence of the weir) 155.65 m and 156.00 m.

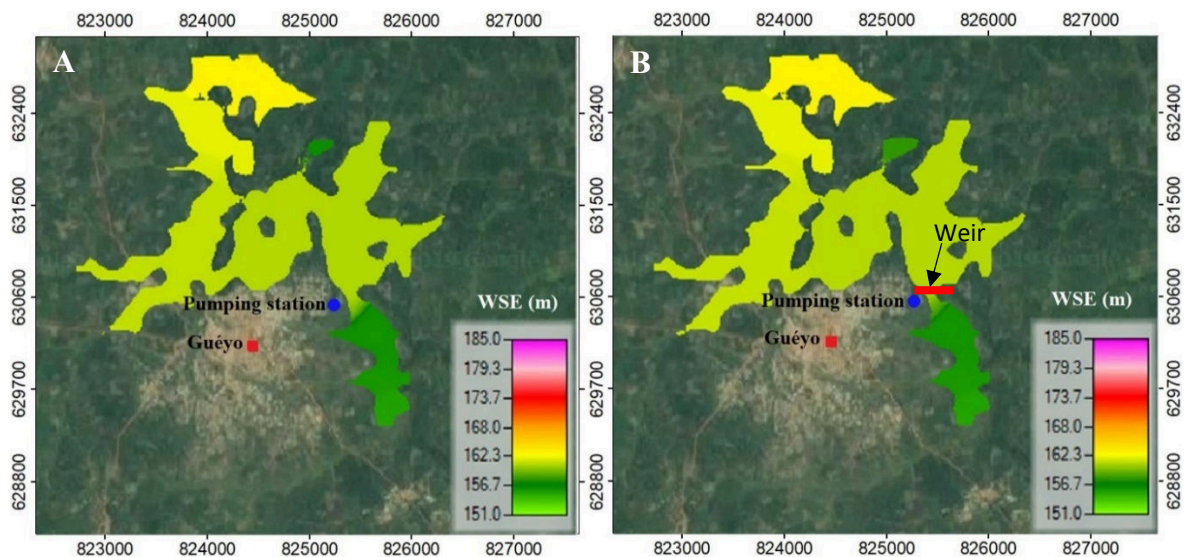


Fig. 8. Water surface elevation before (A) and after (B) the insertion of the weir for the 20 years return periods

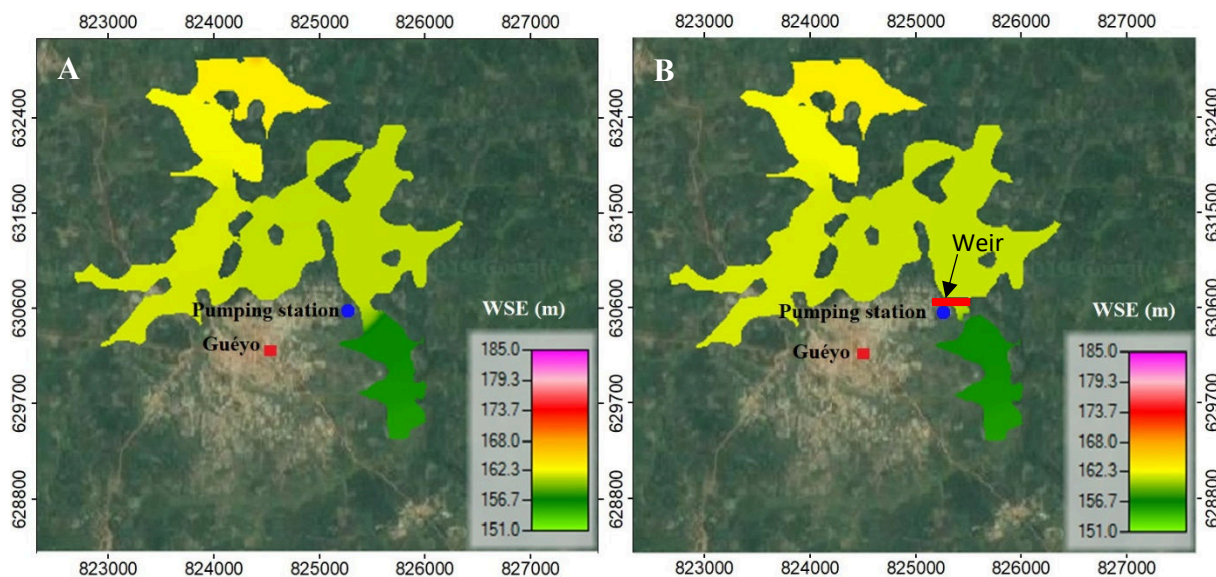


Fig. 9. Water surface elevation before (A) and after (B) the insertion of the weir for the 100 years return period

Table 7 shows the difference between the water levels before and after the insertion of the weir. The small difference in water levels observed shows that the influence of the weir on stream dynamics is negligible because of its judiciously calculated height.

Table 7. Difference between water levels before and after insertion of the weir

Return periods	In the reservoir (m)	Downstream the weir (m)	Difference of WSE in the reservoir (m)	Difference of WSE downstream the weir (m)
20 years	160.75	160.65	0.1	-0.09
100 years	161.06	160.93	0.13	-0.1

4.2 DISCUSSION

Flood propagation modelling of the Davo River using the HEC-RAS 2D Hydrodynamic model simulated water levels, water depths and surfaces that could be flooded in the vicinity of the perimeters of the drinking water treatment plant in the city of Gueyo. The presence of the weir creates an elevation of the water line upstream of the weir, which can lead to the creation of a small water body (670,800 m³) upstream of the structure, followed by an area of rapids on the downstream facing, as shown in [14]'s study. The results showed that the model reproduces the flow conditions of the environment well because the Nash coefficients obtained are greater than 60% [15].

The Manning coefficient used for model calibration is 0.05 s/m^{1/3}. This value is high, but acceptable, due to the sinuosity of the watercourse and the roughness of the bed. These results confirm those of many researchers [11], [16], [17], [18], which indicate that the Manning coefficient is generally high for streams with several meanders and shoreline vegetation such as the Davo River watershed.

The simulation of the flows from the different return periods shows different water levels, but does not reach the location of the treatment plant and the city. The low variation in water levels after simulation with and without the weir is due to the low weir height and also the type of weir (run-of-river dam) to minimize the risk of flooding.

5 CONCLUSION

This study focused on the sizing of a weir and its influence on the propagation of floods from the Davo River at the drinking water production plant in Guéyo (South-West Côte d'Ivoire).

To achieve this, this work has two objectives. The first focused on determining the better dimensions of a run-of-river dam. This resulted in a weir height of 2.5 m, a crest width of 1.3 m, a right-of-way of 3.8 m and a length of 177 m. The weir thus

dimensioned makes it possible to have a usable reservoir and to meet the needs of the population estimated at 0.19 m³/s, or 16,800 m³/day, in all seasons. The second objective was to simulate the dynamics of the Davo River before and after the weir was inserted. The purpose of this simulation was to determine the height of the weir so as not to modify significantly the extent of the floodplain of the Davo River.

RÉFÉRENCES

- [1] Kouakou K. E., Goula B. T. A. & Savané I. (2007). Impacts de la variabilité climatique sur les ressources en eau de surface en zone tropicale humide : Cas du bassin versant transfrontalier de la Comoé (Côte d'Ivoire - Burkina Faso). *European Journal of Scientific Research*, 16 (1) : 31-43.
- [2] Kouakou K. E. (2011). Impacts de la variabilité climatique et du changement climatique sur les ressources en eau en Afrique de l'Ouest : Cas du bassin versant de la Comoé. Thèse Unique de Doctorat, Université Abobo-Adjamé (Côte d'Ivoire), 186 p.
- [3] Yao A. B., Goula B. T. A., Kouadio Z. A., Kouakou K. E., Kane A. & Sambou S. (2012). Analyse de la variabilité climatique et quantification des ressources en eau en zone tropicale humide : cas du bassin versant de la Lobo au Centre-Ouest de la Côte d'Ivoire. *Revue Ivoirienne des Sciences et Technologie*, 19 : 136-157.
- [4] Kouassi A. M., Kouamé K. F., Saley M. B. & Biemi J. (2013). Application du modèle de maillet à l'étude des impacts des changements climatiques sur les ressources en eau en Afrique de l'Ouest: Cas du bassin versant du N'Zi-Bandama (Cote d'Ivoire). *Journal of Asian Scientific Research*, 3 (2) :214-228.
- [5] Rosier B., Boillat J-L. & Schleiss AJ (2010) Semi-empirical model for channel bed evolution due to lateral discharge withdrawal. *Journal of Hydraulic Research* 48, 161–168. <https://doi.org/10.1080/00221681003704129>.
- [6] Barredo J. (2007) Major flood disaster in Europe: 1950-2005. *Natural Hazards* 42, 125–148.
- [7] Bogdanowicz E., Strupczewski W. G., Kochanek K. & Markiewicz I. (2014) Flood Risk for Embanked Rivers. *Journal of Geoscience and Environment Protection* 02, 135–143. <https://doi.org/10.4236/gep.2014.23018>.
- [8] Farina G., Bolognesi M., Alvisi S., Franchini M., Pellegrinelli A. & Russo P. (2017) Estimating discharge in drainage channels through measurements of surface velocity alone: A case study. *Flow Measurement and Instrumentation* 54, 205–209. <https://doi.org/10.1016/j.flowmeasinst.2017.02.006>.
- [9] Kane S., Sambou S., Leye I., Diedhiou R., Tamba S., Cisse MT., Ndione D. M. & Sane M. L. (2017) Modeling of Unsteady Flow through Junction in Rectangular Channels: Impact of Model Junction in the Downstream Channel Hydrograph. *Computational Water, Energy, and Environmental Engineering* 06, 304–319. <https://doi.org/10.4236/cweee.2017.63020>.
- [10] Shafizadeh-Moghadam H., Valavi R., Shahabi H., Chapi K. & Shirzadi A. (2018) Novel forecasting approaches using combination of machine learning and statistical models for flood susceptibility mapping. *Journal of Environmental Management* 217, 1–11. <https://doi.org/10.1016/j.jenvman.2018.03.089>.
- [11] Chow V. T. (1959). *Open Channel Hydraulics*. Mcgraw hill company, Illinois (USA), 245p.
- [12] HEC-RAS (2016). *Analyses river system, Hydraulic reference manual, Version 5.0.4: 50 -251*.
- [13] Sitaram, N. & Rao A. R. (2005). Manning's roughness coefficient in alluvial channels affected by seepage. *ISH Journal of Hydraulic Engineering* 11, 116–124. [Doi:10.1080/09715010.2005.10514806](https://doi.org/10.1080/09715010.2005.10514806).
- [14] Sandre, (2014). *Description des ouvrages faisant obstacles à l'écoulement Sandre (version 1.2) France 15 rue Edouard Chamberland 87065 LIMOGES Cedex (<http://www.sandre.eaufrance.fr>), 80p*.
- [15] Koffi Y. B., Lasm T., Ayrat P. A., Anne J., Kouassi A. M., Assidjo E. & Biemi J. (2007). Optimization of Multi-layers Perceptions models with algorithms of first and second order. Application to the modelling of rainfall-rainoff relation in Bandama Blanc catchment (north of Ivory Coast). *European Journal of Scientific Research*, 17 (3) : 13-328.
- [16] Kasuri L. (2013). Modeling for ecosystem restoration hydrodynamic modelling of Yolo bypass using HEC-RAS. Master of sciences in civil engineering, University of California (USA), 25p.
- [17] Soualmia A., Gharbi M., Dartrus D. & Masbernat L. (2013). Comparison of 1D and 2D hydraulic model for floods simulation on the medjerda river in tunisia. *Journal mater*, 7: 3017-3026.
- [18] Kouassi K. L., Brou L. A., Yao A. B., Kouadio Z. A., Konan K. S., Konan K. F., Koffi B. (2019). 1D-2D Hydraulic Modeling of a Diversion Channel on the Cavally River in Zouan-Hounien, Côte d'Ivoire. *Journal of Water Resource and Protection*, 11:1036-1048; <https://doi.org/10.4236/jwarp.2019.118061>.